Korean Membrane Journal
Vol. 1, No. 1, December, 1999, 25-37

Free Volume in Polymers. Note II°: Positron Annihilation Lifetime Spectroscopy and Applications

G. Consolati, M. Pegoraro[1], and L. Zanderighi[2]

Istituto Nazionale per la Fisica della Materia, Dipartimento di Fisica - Politecnico di Milano - Campus Leonardo - P.za Leonardo da Vinci 32 - Milano - Italy

[1]Dipartimento di Chimica Industriale ed Ingegneria Chimica - Politecnico di Milano - P.za Leonardo da Vinci 32 - Milano - Italy

[2]Dipartimento di Chimica Fisica ed Elettrochimica - Università degli studi di Milano - Via Golgi 19 - 20133 Milano - Italy

(Received October 27, 1999)

Abstract : Positron Annihilation Lifetime Spectroscopy has been extensively applied in recent years to investigate the free volume in polymers, owing to the capability of the electron-positron bound system (positronium) to probe the typical size of sub-nanometric cavities among the macromolecular chains. In this paper we show recent results obtained through this technique in some amorphous polymeric membranes (polyurethanes. PUs, and polytrimethilsylilpropine, PTMSP), after a brief survey of the general features of the annihilation process, as well as of the experimental apparatus. Lifetime of o-Ps decay (τ_3) in PUs increases going from sub T_g to over T_g temperatures, following a sigmoid curve. The corresponding radius and hole mean volume increases with a rate increasing until T_g and than decreasing over T_g. This rate decrement distinguishes the behavior of network polymers from the usual behavior of linear polymers, which have not flex points. This is probably due to lower possibility to reach the glass equilibrium for polymers characterized by a high crosslinking density. The coefficient of dilatation of the free volume fraction is shown to be the sum of two contributes due to the variation with T of the number of holes and of their mean volume. PAL spectrum of PTMSP freshly prepared shows four lifetime components; τ_3 and τ_4. only are useful for free volume study. Two kinds of holes of different equivalent radius are reported ($r_3 \cong 0.460$ nm and $r_4 \cong 0.754$). The equivalent volume does not change in a range of 100 K. However the physical aging increases density and decreases oxygen permeability while r_3 goes down to 0.374 and r_4 to 0.735. The number of holes, obtained from the intensities I_3 and I_4 of PAL spectra, decreases with aging 21.7% and 3.5% for large and small holes respectively.

1. Introduction

A positron injected into a non-metallic solid from a radioactive source, after a fast slowing-down requiring some picoseconds at most [1], becomes thermalized and is strongly attracted by the electrons of the medium. Eventually, annihilation between positron and one of the surrounding electrons takes place: the pair disappears with production of two - or, much more rarely, three photons. However, before this last event, the positron can be involved in a short although complex history: for instance, it can be annihilated into microscopic domains characterized by different electron densities (amorphous and crystalline regions, various kinds of defects, etc.). Moreover, it

can form, with an electron of the medium, a bound system that is called positronium (Ps). The result is a positron annihilation spectrum with different components, whose study is potentially useful to obtain information on the structure of the host medium. In the case of the positron annihilation lifetime spectroscopy (PALS), the most common positron technique, a timing spectrum is typically formed by three components, corresponding to annihilations from ortho-Ps, *o*-Ps (τ_3), from free positrons (τ_2) and from para-Ps, *p*-Ps (τ_1), in order of decreasing lifetime. Ps formation in a polymer takes place in the free volume holes [2], and the spectral component associated to *o*-Ps is particularly sensitive to variations in the number as well as in the size of the holes. Furthermore, analysis in terms of a continuous distribution of Ps lifetimes allows one to get insight into the dispersion of the hole size around their average values.

It has to be pointed out that two kinds of free volume holes could be considered, according to the behavior of the polymers: hard and rigid for glassy polymers and an intermediate state between the glassy and the melt state (liquid-like) for rubbery polymers. In the case of glassy polymers, the local motions of the atoms oscillating in a cage of their neighbors create some 'free volume' in the empty spaces of random packed materials. Since the amplitude of the atom oscillations increases with temperature this free volume also has to increase with temperature in a manner similar to the thermal expansion of the glassy polymer (bulk expansion coefficient). On the other hand, in rubbery materials chain rotational movements, which involve many monomeric units (in the case of polyurethanes about 15 monomeric units), dominate and the free volume holes are strictly related to these movements.

Another aspect related to the PALS techinique is the lifetime of a Ps trapped in a hole with respect to the period of atomic oscillations or of the rotational movements of the chains and with respect to the lifetime of the holes. The period of the swinging of the monomeric units is of the order of 10^{-12} s [3], that is, 100 to 1000 lower than typical Ps lifetimes. This means that during its mean life a Ps is able to evaluate the mean diameter of the hole. The lifetime of a hole may be estimated to be of the same order of magnitude of polymer relaxation time, that is, of the time necessary for the chains to change their conformation, disentangle or slide over one another, and so on. For polymers just around T_g the relaxation time is of the order of magnitude of seconds (sometimes of hours), that is, at least nine orders of magnitude higher than the lifetime of *o*-Ps. Therefore, due to the chain dynamics in rubbery polymers holes are formed and destroyed is such a way that their mean number and mean size are constant during the mean life of Ps.

In the present paper PALS studies of polyurethanes (PUs) and polytrimethilsylilpropine (PTMSP) are reported.

2. Materials and Procedure in the Case of PALS Technique

2.1. PU and PTMSP Preparation

Polyurethanes (PU) (polyether based) were syntetized [4] in two step:

a) preparation of prepolymers by reacting TDI and polyoxypropilene glycols of different length (MW 400, 1200, 2000) with ratio NCO/OH=2;
b) reacting prepolymers with triisopropanol amine (TIPA) to obtain a network. The polymer T_g decreases on increasing the MW of the diols. The structure of the polymer is amorphous: hard domains due to OCONH groups are present even in the rubbery state.

Poly-1-1trimethylsilylpropine (PTMSP) was prepared [5] with $TaCl_5$ in toluene according to Masuda [6], and it was separated from the catalyst by treating the reacted mixture with methanol. The precipitate was dissolved in toluene and re-precipitated with methanol in order to get high purity product.

2.2. Experimental Details of PALS Technique

Positrons, the antiparticles of electrons, are generally produced through the β^+ decay of some

radionuclides. In the presence of electrons they give rise to the annihilation process: the electron-positron pair disappears and a certain number of photons are produced, with the prescription that energy and linear momentum must be conserved. The most probable processes are those involving the creation of two or three photons; their probability depends on the relative spin states of the two particles (singlet states produce an even number of photons, whilst triplet states generate an odd number of quanta). The cross section for the annihilation process into two quanta is more than two orders of magnitude higher than that into three photons.

Among the various available radionuclides ^{22}Na emits a γ ray with a definite energy (1.274 MeV) simultaneously to the positron; therefore, the detection of this photon gives information about the instant of emission of the positron ('start' signal). If only the two quanta annihilation events are considered and one of the two photons is detected, one gets also information on the annihilation instant ('stop'). The delay between the start and stop events measures the life of that particular positron. By collecting a suitable number of such events we will obtain the annihilation timing spectrum, that is, the number of positron which live within a particular time interval. According to the law of the radioactive decay, we expect a spectrum which is exponentially decreasing with time, whence it is possible to obtain the average lifetime (or simply lifetime) of the positron in a particular medium. In fact, the result is much more complex: different lifetimes are generally supplied by an annihilation timing spectrum, since positrons can be annihilated from regions with different electron densities. Indeed, the rich amount of information given by PALS is due to the fact that positron is very sensitive to small changes of the density of the electrons surrounding it. Based on this concept, defects in metallic systems have been studied for many years by means of the various positrons spectroscopies, which furthermore made possible the identification of different kinds of defects in semiconductors.

A simple timing spectrometer is schematically shown in Fig. 1: the start and stop photons are revealed by the two scintillators (SC) and the photomultiplier tubes (PTM) transform the signals into electric pulses. The pulse outgoing from the anode of the photomultiplier is then analysed by the constant fraction discriminator (CFD), which filters the signals through suitable preselected energy windows. If the processed signal satisfies the energy requirements, the discriminator supplies a timing pulse which is received at the input of the time-to-amplitude converter (TAC). This instrument generates a signal linearly increasing with time, whenever a start pulse is collected; the signal is blocked when a stop pulse appears at the input of the TAC. Its output is an analog voltage signal, proportional to the delay between the start and the stop pulses: therefore, it measures the life of the positron. After digitalization and classification through an analog-to-digital converter (ADC), the signal is stored into a multichannel analyzer (MCA), which supplies, for each channel, the number of decays occurring between the instants t and $t + \Delta t$ (if Δt is the width of the channel), that is, the annihilation time spectrum. The quality factor of a timing spectrometer is the resolution, generally defined as the Full Width at Half Maximum (FWHM) of a

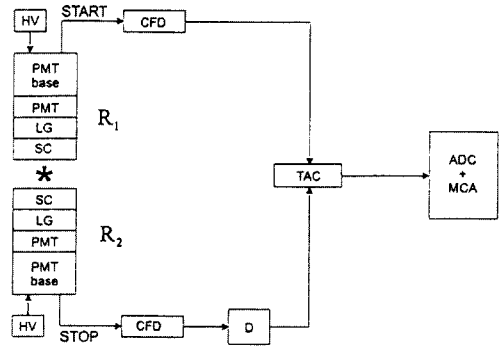

Fig. 1. Schematic drawing of the experimental setup. SC: scintillator; LG: light guide (when necessary); PMT: photomultiplier tube; HV: high voltage; CFD: constant fraction discriminator; TAC: time-to-amplitude converter; ADC: analog-to-digital converter; MCA: multichannel analyzer.

'prompt' curve, corresponding to the registration of two simultaneous events. It mainly depends on the scintillators; values between 200 and 400 ps are quite common.

When the data collection is completed, the annihilation time spectrum is analysed through one of the computer codes nowadays available: the background is subtracted and a deconvolution is carried out (once the resolution function is known) into elemental components. The program supplies also the goodness of the fit, given by a chi-square test. Each component is assumed to be a function exponentially decreasing with time, characterized by a lifetime τ_i and by an intensity I_i which measures the fraction of decays corresponding to a specific annihilation process. In the simplest cases the spectrum $s(t)$ is represented by the following formula:

$$s(t) = \sum_{i=1}^{N} \frac{I_i}{\tau_i} \exp(-t/\tau_i) + b \qquad (1)$$

where b is the background, N is the number of components. This approach is based on the fact that the positron, injected into the sample with high average energy (about 200 keV), thermalizes in a very short time interval and during its subsequent diffusion into the material finds an electron density almost constant with time. If various kinds of defects are present in the medium, the particle can find an electron density lower than the bulk and its lifetime increases. This justifies the presence of different components in eq. (1). In particular, in a macromolecular medium the nanoholes forming the free volume can efficiently host Ps: o-Ps so trapped into a hole decays through a collisional mechanism with the walls of the cavity, by picking one of the valence electrons in relative state of singlet with respect to the positron ('pickoff' mechanism). On the other hand, p-Ps mainly decays with its own electron and its lifetime is scarcely dependent on the structure of the medium. For this reason, PALS applications to polymers are mostly concerned with o-Ps components. It follows that o-Ps lifetime is correlated to the typical dimensions of the hole, in the sense that the lifetime increases when holes expand.

The mean size of the holes forming the free volume can be roughly estimated by means of a simple quantum mechanical model [7,8]: o-Ps in a hole is approximated to a particle in a spherical potential well with radius R_o. It is assumed that an electronic layer forming a thickness δR is present on the walls of the hole, whose effective radius is consequently $R=R_o-\delta R$. The following equation relating R (Å) and τ_3 (ns) is obtained:

$$\tau_3^{-1}=2[1-R/R_o+0.159 \sin(2\pi R/R_o)] \qquad (2)$$

If we accept for R the value 1.66 Å - obtained by fitting positron annihilation data in porous materials of known hole size [9], the semi empirical equation (2) allows one to find the average volume of the hole $v_h=4\pi R^3/3$, in spherical approximation. Of course, the model is rather rough, since real cavities have irregular shapes; therefore, the radii must be interpreted only as typical sizes. However, the order of magnitude and the behavior of the nanovolumes with specific quantities (like temperature, pressure or mechanical stress) is expected to be correct. Since the nanoholes do not show the same dimensions, but rather display a distribution of volumes, we can suppose that o-Ps exhibits a corresponding distribution of lifetimes. Consequently, a distribution of o-Ps lifetimes as a result of a deconvolution of the annihilation time spectrum allows one to get information about the hole volume density distribution, even though in sperical approximation. In the last years new algorithms appeared, which are able to supply such lifetime distributions using different mathematical approaches [10-12]. The comparison between the results obtained by PALS measurements and the distribution of free volume predicted e.g. by the Simha-Somcynsky theory in polystyrene [13] produced a remarkable agreement.

Concerning o-Ps intensity I_3, it is generally assumed that it contains information related to the number of the free volume holes, although the agreement on this point is anything but general [14,15]. The simplest guess is a linear correlation between intensity and hole concentration [16,17]; in

such a case the free volume can be written as:

$$V_f = CI_3 v_h \quad (3)$$

where C is a constant which can be determined by calibration, using another technique [2]. For polymers in the glassy state it is found that I_3 depends on the cooling rate of the sample: it is higher, the higher is the rate of cooling [18]. Such behaviour sheds some shadows on the physical meaning of this parameter, but is consistent with the non-stationary behavior of the glassy state and it is an indirect argument in favour of using Ps as a detector ('seeker') of free-volume holes.

3. Results and Discussion

3.1. Polyurethane Structure and Characterization

From a fundamental point of view, PUs are characterized by the presence of various chemical groups. Indeed, altering the nature of the reagents and the molecular weight of the non-isocyanate components, their chemical composition and the relative concentration of the chemical groups may be changed. The modification of the chain composition changes the physico-chemical properties of the polymer, such as the glass transition temperature, the concentration of the hard or soft zone, etc., mainly because of the different hydrogen bond density.

Even when PUs appear amorphous from X-ray and DSC analysis, short-range order is still possible. In both linear and cross-linked PUs the hydrogen bond interactions between the urethane groups present in different chains are responsible for the formation of short-range regions that segregate into the so-called 'hard' domains. The long chains between urethane groups, consisting of flexible oligomeric diols or diamine, bind the 'hard' zones, forming 'soft' domains where the interaction forces among the chains are 'soft' and of the van der Waals type, and allow the free movements of the chains when the polymer is above T_g.

PALS data on some amorphous cross-linked polyurethanes are reported, in the temperature interval 100-400 K, which contains the temperature range for the normal use of these polymers (280-370 K). In this interval, a glass transition and, possibly, transitions due to the breaking of the hydrogen bonds between soft and hard zones, may be present.

3.1.2. Nanoholes Volumes in PUs

The timing spectra were resolved into three components, by assuming the two shortest lifetimes to be discrete, whilst the longest component was allowed to be a distribution of lifetimes. According to the common interpretation the lifetimes τ_1 and τ_2 are associated to annihilation of positrons not forming bound states, but localized into regions characterized by different electron densities. τ_1 should be considered as a weighted mean of two different components, since it contains annihilations from p-Ps and the distributed lifetime of the longest component τ_3 is attributed to o-Ps decay.

The trend of $\bar{\tau}_3$, centroid of the lifetime distribution of the longest components *versus* the temperature, is shown in Fig. 2 for the PU 400, PU 1200, PU 2000 which are characterized, respectively, by molecular masses between the cross-links of 907, 1706 and 2657 Dalton; a monotonic increase is observed, which is very similar for the various samples. Three temperature regions can be distinguished: the 'low', and 'high' temperature

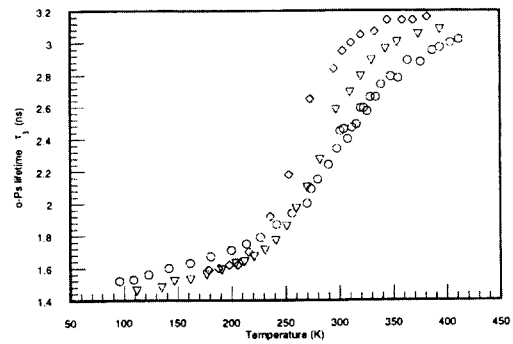

Fig. 2. o-Ps lifetime (ns) for the different investigated PS as a function of temperature (K): ○, molecular weight 400; ▽, molecular weight 1200; ◇, molecular weight 2000.

regions (T < 200 K and T > 320 K, respectively) where there is a moderate variation of $\bar{\tau}_3$ with T, and the 'intermediate' region where a sharp increase of the rate of variation of $\bar{\tau}_3$ with T is evidenced. The change in the $\bar{\tau}_3$ variation between 'low' and 'intermediate' temperatures is associated with some morphological transition since o-Ps lifetime is sensitive to the electron density surrounding Ps and, therefore, to the size of the free volume holes.

For low T the molecular movements of the polymer chains in the 'soft' domains are 'frozen in' (glassy state) by the van der Waals forces among the chains, only small fluctuations are allowed and the free space around the chains is small: any increase of T produces small effects on the thermal motion of the polymer chains and, consequently, only a small increase of the free volume, that is, of the size of the free volume holes. Therefore small variations of τ_3 *versus* the temperature must be expected, according to the reported data.

On the other hand, by increasing the temperature the thermal movements of the chains segments also increase, and at a given value of T the fluctuation energy becomes of the same order of the interaction energy. In this condition the amplitude of the fluctuations may increase followed by an increase of the free volume around the chains. The temperature at which this phenomenon occurs is called glass transition temperature T_g, since this temperature marks the 'glassy state' ↔ 'rubbery state' transition of the soft fraction of the PUs.

For T > T_g the soft polymer fraction is in a rubbery state, the increased mobility of the chains and the average size of the holes both increase with temperature. Therefore o-Ps lifetime also shows an increased variation with the temperature. In the region of 'high' temperatures a decrease in the rate of variation of $\bar{\tau}_3$ with temperature, $d\bar{\tau}_3/dT$, is evident. A possible explanation is related to the presence of the cross-linking: it can be reasonably guessed that cross-linking somehow constrains the movements of the polymer segments, by preventing the hole volume to increase at the same rate as in the absence of cross-links. It seems possible that the hole volume of the polymer is constrained

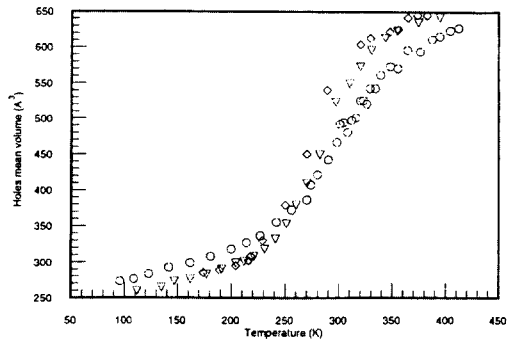

Fig. 3. Dependence on the temperature (K) of the average volume of the holes ($Å^3$) in PU membranes with molecular weight PU 400, 1200, 2000. The symbols have the same meaning as in Fig. 2.

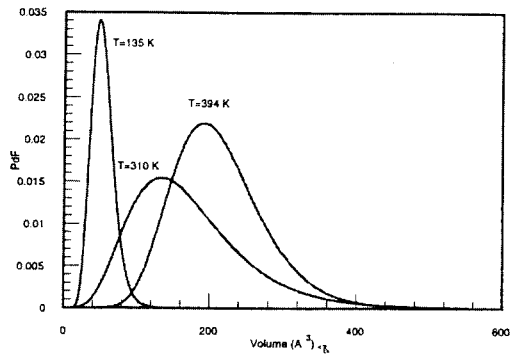

Fig. 4. Probability density function of hole volumes for PU 1200 at some selected temperatures.

by cross- links at T > T_g. A similar behavior was already shown in an amine-cured epoxy polymer [19]. Fig. 3 shows the average hole volume v_h in the investigated PUs at the various temperatures.

From the lifetime distribution it is possible to obtain the hole volume distribution function, which is shown in Fig. 4 for PU 1200 as an example at some selected temperatures. The hole volume distribution shows an increased dispersion, Δ_3, going from T < T_g to T > T_g reflecting the higher freedom of movements of the macromolecular segments, which means an average increase in the size of the holes but also an increase of the dispersion in their volume around the mean value. Indeed, it is reasonable to suppose that the various

molecular motions require different expenditures of energy, and consequently are achieved in different amounts, at fixed temperature.

Owing to the hindrance of the enlargment of the free volume holes at high temperature, such as by cross-links, the larger holes will stabilize themselves whilst the volume of the smaller holes will grow with temperature. This fact implies an increase of the mean volume of the holes, and therefore of $\bar{\tau}_3$, that must be correlated to a decrease in the hole dispersion, owing to the decrease of the number of small holes, while the volume of large holes remains constant. All this is supported by the decrease of Δ_3, as shown in Fig. 4. In agreement with the previous analysis the variation of the hole distribution with temperature should strongly depend on the presence and nature of chain interaction.

3.1.3. o-Ps Intensity and Hole Densities

For a family of materials characterized by a similar electron distribution, the intensity of the longest component, I_3, is generally correlated to the density of holes N_h that can be considered as a kind of trapping centers for Ps.

In Fig. 5 the intensity I_3 is shown as a function of the temperature, for all the investigated PUs. Three temperature regions corresponding to the change in the I_3 trend can be distinguished: in the low temperature region the intensity I_3 linearly increases with T. Near T_g and above it, I_3 remains constant, for a region roughly corresponding to the 'rise' of $\bar{\tau}$; at 'high' T, I_3 starts to increase again.

The interpretation of this experimental data, according to the above-mentioned assumption, is that the density of holes increases linearly with the temperature when the polymer is in the glass-like state; it becomes constant in the temperature interval (T_g, $T_g+\Delta T$); then, it starts to increase at the highest temperatures. It is difficult to properly explain the increase of I_3 beyond the plateau. However, it may be suggested that the hydrogen bonds of the hard domains, present in an amorphous matrix, could be destroyed by heating the polymer above T_g [20]: in this event the polymer segments reach further mobility and hole formation

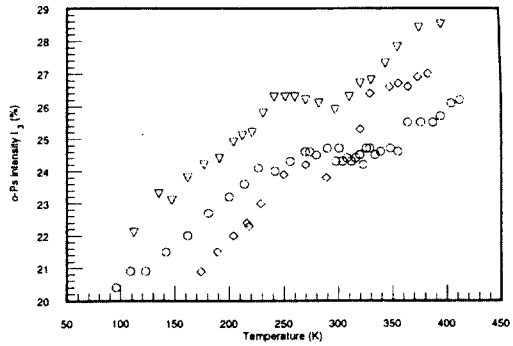

Fig. 5. o-Ps intensity (%) for the investigated PU against the temperature (K). The symbols have the same meaning as in Fig. 2.

is favored. The DSC of PU 400, when performed at high heating rates (0.33 K/s), shows a small thermal effect at around 340 K that could be attributed to hydrogen bond breaking. The values of ΔT for the plateau depend on the polymer and the following values can be measured: $\Delta T_{PU400} \cong 100$ K; $\Delta T_{PU1200} \cong 75$ K; $\Delta T_{PU2000} \cong 50$ K: it is quite easy to remark that the temperature interval where I_3 is constant increases with the density of cross-linking. The trend in the I_3 values adds information to the previous discussion on the hole volume behavior throughout the glass transition temperature: the transition from the glassy state to a rubber-like state not only implies a strong increase of the amplitude of the motion at molecular scale but also a limit to the increase in the number of holes. In the case of the PU studied, the thermal energy given to the system in the neighborhood of T_g will be distributed mainly to increase the volume of the holes, not their number.

3.1.4. Free Volume Fraction and Thermal Expansion Coefficient in PU

The fractional free volume $f(T)$ at the different temperatures can be evaluated from the reported data by assuming V_f to be proportional both to the density of holes and to the average volume of each hole, according to eq. 3:

$$f(T) = \frac{V_f}{V_t} = \frac{N_h V_h}{V_t} = \frac{C I_3(T) V_h(T)}{V_t} \quad (4)$$

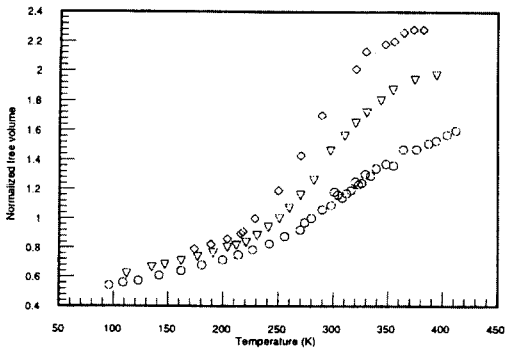

Fig. 6. Normalised fractional free volume ($f(T)/f(T_g)$)in the different PU networks as a function of temperature (K). Symbols have the same meaning as in Fig. 2

The values of $f(T)/f(T_g)$ versus T are reported in Fig. 6 for the different PUs; we can observe a sigmoid behavior, with markedly different slopes above, below and in the central region of the glass transition. The functional dependence of $f(T)$ on T is partially in agreement with the Williams, Landel and Ferry [21] (W.L.F.) free volume theory, which predict that going beyond the T_g region, the free volume changes from a constant value (2.5% of the specific volume) at $T \leq T_g$ to high values which increase linearly with $\Delta T = T - T_g$ and the dilatation coefficient of the free volume, $\alpha_f = (1/V_f)(dV_f/dT)$, is about twice the dilatation coefficient of the glassy phase. The W.L.F. equation is accepted above T_g. Below T_g free volume is assumed not to be constant but to change slowly as a function of T and of the duration of the experiment.

The total volume V_t of a polymer may be expressed as the sum of the occupied volume V_o and the free volume V_f. The thermal expansion coefficient α_v is defined as:

$$\alpha_v = \frac{1}{V_t}\frac{dV_t}{dT} = \frac{dln(V_t)}{dT} = \frac{dln[V_o(1+V_f/V_o)]}{dT} \qquad (5)$$

$$\alpha_v = \alpha_o + \frac{d}{dT}\left(\frac{V_f}{V_o}\right)$$

where $\alpha_o = (1/V_o)(dV_o/dT)$ is the thermal expansion coefficient of the occupied volume (or van der Waals volume); in the last passage it is supposed $V_f < V_o$.

By developing the derivative one gets:

$$\alpha_v = \alpha_o \frac{1-2f}{1-f} + \alpha_f \frac{f}{1-f} \qquad (6)$$

which, by taking only linear terms in f, assumes the following expression:

$$\alpha_v = \alpha_o(1-f) + f\alpha_f \qquad (7)$$

The first term at the second member is the contribution to the volumetric expansion coefficient due to the volume occupied by the atoms while the second one is the contribution due to the free volume.

According to the equation (3) and the definition of α_f one gets:

$$\alpha_f = \left[\frac{d\ln I_3}{dT} + \frac{d\ln V_h}{dT}\right] = \beta_I + \alpha_h \qquad (8)$$

The contributions to the free volume expansion coefficient are due to the variation of the number of holes (β_I) and of the hole volume (α_h) and are reported in Table 1. The behavior of α_h and β_I is different for the various temperature ranges. At $T < T_g$, $\alpha_h > \beta_I$; on the other hand, in the intermediate temperature range, α_h increases whilst β_I is zero; indeed, according to the previous discussion the glass transition region is characterised by the increase of the hole volume, the number of holes remaining constant. At higher temperatures, the hole volume contribution α_h decreases to values lower than those found in the glassy state, conversely β_I assumes the values found at low temperature range.

According to the W.L.F. theory at $T = T_g$ the free volume fraction is equal for all solids: $f(T_g) = 0.025$. By assuming that this value holds also near around the T_g value, one gets the values of the contribution of the free volume expansion coefficients, $f\alpha_f$ (Table 2), to the volume expansion coefficient. The values reported in Table 2 are in

Table 1. Thermal Coefficient (K^{-1}) for the Holes α_h and for the Hole Density β_I Evaluated in Different Temperature Ranges. All the Values have been Multiplied by 10^3 [4]

	Low temperature		Middle temperature		High temperature	
	α_h	β_I	α_h	β_I	α_h	β_I
PU400	4.0	1.1	7.4	-	3.0	1.1
PU1200	2.8	1.2	10.3	-	0.7	1.3
PU2000	2.9	1.3	13.0	-	0.7	1.5

Table 2. Contribution to the Thermal Expansion Coefficient α_v of the Free Volume $\alpha_f \times 10^4$ Evaluated in Different Temperature Ranges for the PUs Studied [4]

	Low temperature	Middle temperature	High temperature
PU400	1.3	1.8	1.0
PU1200	1.0	2.6	0.5
PU2000	1.1	3.2	0.6

the range of the volume expansion coefficient for polymers.

3.2. Glassy Polymers: the Case of PTMSP

3.2.1. PTMSP Structure and Characterization

DSC analysis has shown no glass transition of PTMSP until decomposition temperature: this indicates that the polymer chains are very stiff and that with thermal treatment, it is easier to break the chain chemical bonds than to get a mobility of the segments of the polymer chains.

IR data undoubtedly indicate that in air double bonds may react with oxygen, forming some carbonyl groups. Masuda et al. [22] reported that no molecular weight decrease was observed when PTMSP is aged in air at room temperature for a long period of time, and on this basis they conclude that PTMSP does not undergo oxidation. Our IR spectra reveal that oxidation does occur. We suggest that oxidation does not involve a strong chain breaking but an inner rearrangement. The reaction mechanism of this rearrangement has to

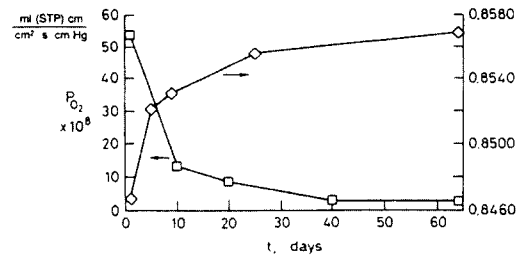

Fig. 7. Change in permeability and density of a PTMSP membrane aged in air vs. time (days).

be investigated.

Aging has no effect on the tensile properties of PTMSP. The elongation at break has a normal value for a glassy polymer, but it is lower than the value reported in the literature [23] (13.36% against 73%). This difference may be due to differences in the preparation procedure. The main effect of aging phenomena is to increase the density and to decrease the permeability of the polymer without any sensible variation in the mechanical properties. The decrease in permeability with aging is already known from the literature [24]. It is interesting to point out that the increase in the density of the polymer in 60 days (from 0.8467 to 0.8569, that is, about 1.2%) is paralleled by the decrease in the permeability (about 17.5 times) (Fig. 7). This decrease may be explained in terms of an inner rearrangement of the chain of the polymer, with the reduction of either the size or the number of free volume holes, or both. To investigate this aspect PALS technique was used; results are shown in the next section.

By using a monomer sequence with a minimum energy (head-tail sequence) we have verified with SASM molecular models (scale 1 cm=10^{-8} cm) that the conformation of the PTMSP chain does not make it possible to obtain full cis- or full trans-sequences, as the steric hindrance allows the formation of sequences with a maximum of three to four monomers in the same configuration (cis or trans). The comparison of a cis- and trans-model suggests that the possible sequence of TMSP in the PTMSP chain is *(cis-cis-cis-trans-)* with

Table 3. Permeability Data of Freshly Prepared PTMSP Membrane mL(STP)*cm/s*cm^2 *cmHg) 10^8

	Our Data [5]	From Literature [26]
Oxygen	53.9	26-77.3
Nitrogen	24.5	15-49.7

formation of a quite rigid chain. This hypotheses agrees with the molecular mechanic and molecular dynamic calculations of Clough et al [25]. These authors have shown that PTMSP has a cis-transoid conformation with small segments of cis-bounded monomers connected with some trans units to form an elicoidal structure. The calculated barriers for rotation about a backbone single bond are approximately 40 kcal/mol [22].

The result of this molecular model investigation is that the conformation is so closed and compact that probably only the double bond of monomers in trans position may be available for the reaction with oxygen. This could justify the appearance in the IR spectra of samples left in air at room temperature for a long period of time, of a peak assigned to C=0 bond and the decrease of the peak assigned to C=C.

3.2.2. PALS Results

The measured PAL spectra were resolved into four discrete components. The experimental values of τ_3 and τ_4 are much higher than the lifetime of *p*-Ps (τ_1=0.12 ns) and of positrons and positron-molecule species ($\tau_2 \cong 0.4$ ns); therefore, they may be reasonably associated to *o*-Ps. Only the two long-lived components, τ_3 and τ_4, are reported in the tables and discussed in the following.

PALS results under vacuum of freshly prepared samples as a function of temperature (Table 4) show, without a trace of doubt, that there are no appreciable variations in the values of lifetime τ_3 and τ_4 and in the relative intensities, at least in the temperature range investigated (297-376 K). This confirms that the configuration of PTMSP is very rigid, as a temperature variation of 79 K does not change the number and the size of the free volume holes.

The stiffness of the chain and some irregularities in the monomer sequences could explain why it is not possible to obtain a regular lattice from a solution of PTMSP by solvent evaporation and also justify the stability of the glass phase at very high temperature.

In a recent experiment [27] we extended the range of investigated temperatures (from 180 to 360 K) and carried out the deconvolutions of timing spectra by considering a distribution of lifetimes for the longest component τ_4. The centroid $\bar{\tau}_4$ remains constant, according to the data displaied in Table 4; Fig. 8 shows the volume distribution of nanoholes at the various temperatures. The dispersion of the distribution of volumes decreases with temperatures, which can be interpreted as an homogenizing of the nanoholes, at higher temperatures. This is reasonable, if the stifness of the macromolecular 'backbone' effectively hinders the increase of the size cavities, due to thermal move-

Table 4. The Two Long-lived Components of PAL Spectra under Vacuum of Freshly prepared PTMSP at Increasing Temperature [5]

T (K)	I_3 (%)	τ_3 (ns)	r_3 (nm)	I_4 (%)	τ_3 (ns)	r_4 (nm)
297	9.7±0.5	4.7±0.3	0.460	31.1±0.6	13.8±0.1	0.754
315	9.0±0.5	4.2±0.3	0.436	32.9±0.6	13.5±0.1	0.748
326	9.9±0.5	4.8±0.3	0.464	32.0±0.6	13.7±0.1	0.753
334	8.7±0.5	4.2±0.3	0.436	33.3±0.6	13.4±0.1	0.745
344	9.2±0.5	4.4±0.3	0.445	33.2±0.6	13.4±0.1	0.746
354	9.4±0.5	4.7±0.3	0.461	33.1±0.6	13.5±0.1	0.747
362	9.4±0.5	4.7±0.3	0.459	33.4±0.6	13.4±0.1	0.745
376	9.6±0.5	4.6±0.3	0.454	33.9±0.7	13.4±0.1	0.745

Table 5. The Two Long-lived Components of PAL Spectra at 297 K in Air and under Vacuum of Freshly prepared PTMSP [5]

P (bar)	I_3 (%)	τ_3 (ns)	r_3 (nm)	$v(\tau_3)(nm)^3$	I_4 (%)	τ_4 (ns)	r_4 (nm)	$v(\tau_4)(nm)^3$
F(1)	11.2±0.5	2.8±0.2			31.1±0.6	6.63±0.07		
A(1)	9.1±0.5	2.2±0.1			26.4±0.5	6.4 ±0.1		
F(10^{-4})	9.7±0.5	4.7±0.3	0.460	0.408	31.1±0.6	13.8 ±0.1	0.754	1.790
A(10^{-4})	9.2±0.5	3.2±0.2	0.374	0.219	25.8±0.5	13.0 ±0.1	0.735	1.670

The numebers in parentesis indicate the oxigen pressure in bar.

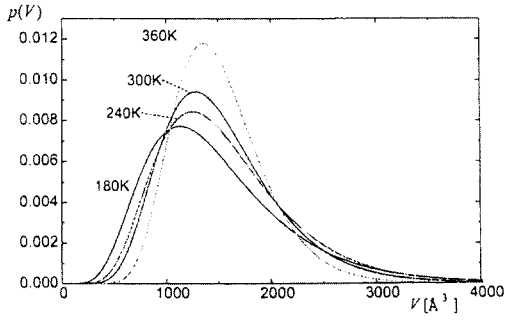

Fig. 8. Volume distributions of nanoholes in PTMSP at different temperatures.

ments.

The effect of oxygen sorption is shown in Table 5; a strong interaction between *o*-Ps and oxygen takes place, both in the fresh (F) and aged (A) samples, which results in a sensitive reduction of *o*-Ps lifetime. This effect must be attributed to a conversion of *o*-Ps into *p*-Ps induced by the paramagnetic oxygen dissolved in the PTMSP and present in the free volume holes. The interpretation is supported by an experiment of magnetic quenching of Ps recently carried out [28].

3.2.3. Analysis of PALS Results

The physical interpretation of the presence of two *o*-Ps lifetimes is still an unsolved problem [29-31]. Different hypotheses have been proposed such as one *o*-Ps in the bulk and another one in the defects of the solid, the presence of amorphous and crystal phases, an effect due to the interphase between amorphous and crystal phases, bounded states of *o*-Ps on the surfaces of holes, etc. As far as PTMSP data are concerned, our opinion is that the two long-lived components may be assigned to *o*-Ps annihilation in two different-sized holes. According to this hypothesis, thermodynamic unstable, or non-equilibrium, pore-like holes, or cages, are present in PTMSP connected with channel-like holes typical of PTMSP structure and due to the rigid backbone chains separated by bulky trimethylsilyl side groups [32].

As a working hypothesis we suggest a bimodal distribution of free volume holes: large cages (mean value of R=0.75 nm) originated from the non- equilibrium state of the glassy polymer and channel- like, or structural, holes (mean values of R=0.45 nm) due to chain-to-chain separation. The values of the effective radii reported in Tables 4 and 5 have been evaluated according to eq.2. The previous hypothesis can be justified as follows. If Ps should be free, it would probe, during its lifetime, a large number of different holes and consequently the lifetime spectrum would exhibit only one long mean lifetime component. Moreover, it is known that the free Ps only exists in crystalline structures, where it is delocalized; on the other hand, in amorphous materials Ps is strongly localized into the defects. Because PTMSP is a glassy polymer, we must expect Ps to be localized around the sites of its formation. Indeed, experiments have shown that Ps localized into defects has a diffusion constant that is orders of magnitude less with respect to free Ps. For instance, in crystalline ice -where Ps is delocalized - D_{Ps}=0.2 $cm^2\ s^{-1}$, whereas in amorphous ice, in the presence of defects, $D_{Ps}=10^{-3}\ cm^2\ s^{-1}$, and decreases by increasing the defects' concentration [33].

By generalizing the previously assumed propor-

tionality between free volume fraction and the product of *o*-Ps intensity and average volume of nanoholes (eq.3) we can write:

$$f=C*(v_3(\tau_3)*I_3+v_4(\tau_4)*I_4)$$

where f is the total free volume fraction of the polymer, C is a constant, and v_i is the average volume of i type hole; C was assumed to be characteristic of *o*-Ps in a medium and not of the holes in the medium. From the data reported in Table 4, the percentage variation of the free volume in 60 days results in 21.2% for PALS measurements on samples in air and 24.3% on samples under vacuum. The two values are in good agreement and a mean value of free volume decrease of 22.7% may be assumed.

From density data, the specific volume variation results as $\Delta v_t=1.185\times10^{-2}$ (mL/mL) and it is equal to the total variation of the free volume f, because the occupied volume cannot change at constant temperature:

$$\Delta v_t=\Delta f$$
$$0.01185\ (\mathrm{mL/mL})=\Delta f\ (\mathrm{mL/mL}).$$

On the other side,

$$\frac{\Delta f}{f}=0.227$$

Therefore, for f one obtains

$$f = 5.22\times10^{-2}.$$

From the data in Table 4 the volume fraction of larger holes is about 4.96×10^{-2} and that for one of the smaller holes is about 0.26×10^{-2}.

From the mean volume of the holes and the fraction of the free volume of small and large holes, it is possible to evaluate the density number N of holes: for freshly prepared samples the density number of large holes is $N^l_f=2.8\times10^{19}$ (mL^{-1}) and for smaller holes it is $N^s_f=0.85\times10^{19}$ (mL^{-1}); for the aged sample the density number for larger holes is $N^l_a=2.3\times10^{19}$ (mL^{-1}) and for smaller ones $N^s_f=0.82\times10^{19}$ (mL^{-1}).

Although the variation of the free volume fraction attributed to the smaller holes is a modest amount of the total variation, we note that the radius of the channels reduces of about 20% from freshly to aged samples; this could be correlated to the strong decrease observed in the permeability of the membrane, if we suppose that the channel-like holes play a critical role in the diffusion of gas molecules throughout the polymer.

References

1. H. Nakanishi and Y. C. Jean, "Positron and Positronium Chemistry," ed. D. M. Shrader and Y. C. Jean. Elsevier, Amsterdam (1988).
2. Y. C. Jean, "Positron and Positronium Chemistry," Y. C. Jean (ed), World Scientific, Singapore (1990).
3. G. Zerbi, R. Magni, M. Gussoni, K. H. Moritz, A. Bigotto and S. Dirlikov, *J. Chem. Phys.*, **75**, 3175 (1981).
4. G. Consolati, J. Kansy, M. Pegoraro, F. Quasso and L. Zanderighi, *Polymer*, **39**, 3491 (1998).
5. G. Consolati, I. Genco, M. Pegoraro and L. Zanderighi, *J. Polym. Sci. part B: Polym. Phys.*, **34**, 357 (1996).
6. T. Masuda, E. Isoba and T. Higashimura, *Macromolecules*, **18**, 841 (1985).
7. S. J. Tao, *J. Chem. Phys.*, **56**, 5499 (1972).
8. M. Eldrup, D. Lightbody and J. N. Sherwood, *Chem. Phys.*, **63**, 51 (1981).
9. H. Nakanishi and Y. Ujihira, *J. Phys. Chem.*, **86**, 4446 (1982).
10. R. B. Gregory and Y. Zhu, *Nucl. Instr. Methods* A **290**, 172 (1990).
11. A. Shukla, M. Peter and L. Hoffmann, *Nucl. Instr. Methods* A **335**, 310 (1993).
12. J. Kansy, *Nucl. Instr. Methods* A **374**, 235 (1996).
13. R. E. Robertson, "Computational Modelling of Polymers," edited by J. Bicerano, Marcel Dekker, New York (1992).
14. V. Shantarovich, *J. Radioanal. Nucl. Chem.*, **210**, 357 (1996).

15. C. L. Wang, T. Hirade, F. H. J. Maurer, M. Eldrup and N. J. Pedersen, *J. Chem. Phys.*, **108**, 4654 (1998).
16. M. Y. Ruan, H. Moaddel, A. M. Jamieson, R. Simha and J. D. McGervey, *Macromolecules*, **25**, 2407 (1992).
17. H. Nakanishi, Y. C. Jean, E. G. Smith and T. C. Sandreczki. *J. Polym. Sci.*, B **27**, 1419 (1989).
18. J. Kristiak, O. Sausa, P. Bandzuch and J. Bartos, *J. Radioanal. Nucl. Chem.* A **210**, 563 (1996).
19. Y. C. Jean, T. C. Sandreczki and D. P. Ames, *J. Pol. Sci.* B **24**, 1247 (1986).
20. A. Tobolsky, "Properties and Structure of Polymers," J. Wiley, N. Y. (1960).
21. M. L. Williams, R. F. Landel and J. D. Ferry, *J. Am. Chem. Soc.*, **77**, 3701 (1955).
22. T. Masuda, B-Z. Tang, T. Higashimura, and H. Yamaoka, *Macromolecules*, **18**, 2369 (1985).
23. T. Masuda, B-Z. Tang, A. Tanaka, and T. Higashimura, *Macromolecules*, **19**, 1459 (1991).
24. T. Hamano, T. Masuda and T. Higashimura, *J. Polym. Sci., Part A, Polym, Chem.*, **26**, 2603 (1988).
25. S. B. Clough, X. F. Sun, S. K. Tripathy and G. L. Baker, *Macromolecules*, **24**, 4264 (1991).
26. N. A. Plate', A. K. Bokarev, N. E. Kaliuzhanyi, E. G. Litvinova, V. S. Khotimskii, V. V. Volkov and Yu. P. Yampol'skii, *J. Memb. Science*, **60**, 13 (1991).
27. G. Consolati, R. Rurali and M. Stefanetti, *Chem. Phys.*, **237**, 493 (1998).
28. G. Consolati and F. Quasso, *Appl. Phys.*, B **66**, 371 (1998).
29. G. Consolati, and F. Quasso, *Appl. Phys.*, **A50**, 43 (1990).
30. Y. Ito, M. Hirose, and Y. Tabata, *Appl. Phys.*, **A50**, 39 (1990).
31. C. Dauwe and M. Kwete, "Positron Annihilation," ed. P. G. Coleman, S. C. Sharma and L.M. Diana, North-Holland, Amsterdam (1982).
32. Y. Ichiraku, S. A. Stern and T. Nakagawa, *J. Membr. Science*, **34**, 5 (1987).
33. M. Eldrup, A. Vehanen, P. J. Shultz, and K. G. Lynn, *Phys. Rev. Science. Lett.*, **51**, 2007 (1983).